Barium-catalysed dehydrocoupling of hydrosilanes and borinic acids: A mechanistic insight

Erwann Le Coz, Ziyun Zhang, Thierry Roisnel, Luigi Cavallo, Laura Falivene, Jean-François Carpentier, Yann Sarazin

10.1002/chem.201904933

Barium-catalysed dehydrocoupling of hydrosilanes and borinic acids: A mechanistic insight

Erwann Le Coz,[†,[a]] Ziyun Zhang,[†,[b]] Thierry Roisnel,[[a]] Luigi Cavallo,[[b]] Laura Falivene,*[[b]] Jean-François Carpentier,[[a]] and Yann Sarazin*[[a]]

[a] Univ Rennes, CNRS, ISCR (Institut des Sciences Chimiques de Rennes) – UMR 6226, F-35000 Rennes (France)
E-mail: yann.sarazin@univ-rennes1.fr

[b] Physical Sciences and Engineering Division, Kaust Catalysis Center, King Abdullah University of Science and Technology (KAUST), Thuwal 23955-6900, Saudi Arabia
E-mail: laura.falivene@kaust.edu.sa

† These two co-authors contributed equally to the work.

Keywords: Barium • dehydrocoupling catalysis • borasiloxane • mechanism • DFT

10.1002/chem.201904933

Abstract

Two very rare cases of barium boryloxides, the homoleptic $[Ba(OB\{CH(SiMe_3)_2\}_2)_2.C_7H_8]$ and the heteroleptic $[\{LO^{NO4}\}BaOB\{CH(SiMe_3)_2\}_2]$ stabilised by the multidentate aminoetherphenolate $\{LO^{NO4}\}^-$, are presented, and their structural properties are discussed. The electron-deficient $[Ba(OB\{CH(SiMe_3)_2\}_2)_2.C_7H_8]$ shows in particular resilient η^6-coordination of the toluene molecule. Together with its amido parents $[Ba\{N(SiMe_3)_2\}_2.thf_2]$ and $[Ba\{N(SiMe_3)_2\}_2]_2$, this complex catalyses the fast and chemoselective dehydrocoupling of borinic acids R_2BOH and hydrosilanes $HSiR'_3$, yielding borasiloxanes $R_2BOSiR'_3$ in controlled fashion. The assessment of substrate scope indicates that, for now, the reaction is limited to bulky borinic acids. Kinetic analysis was performed, showing that the rate-limiting step of the catalytic manifolds traverses a dinuclear transition state. A detailed mechanistic scenario is proposed on the basis of DFT computations, the results of which are fully consistent with experimental data. It consists of a stepwise process with rate-determining nucleophilic attack of a metal-bound O-atom onto the incoming hydrosilane, involving throughout dinuclear catalytically active species.

10.1002/chem.201904933

Introduction

Along with other main block elements,[1] the large alkaline earth (Ae) metals calcium, strontium and barium have been attracting wide interest as viable alternatives to expensive, and often toxic, late transition metals, in order to devise molecular (pre)catalysts implemented in a variety of organic transformations.[2-5] Ae-based catalytic systems show overall excellent performances in reactions such as the hydroelementations of unsaturated carbon-carbon,[6-15] C=N[16] or C=O bonds,[17-19] as well as polymerisations[20-24] and dehydrocouplings.[23-29] Beyond their large size, the originality of Ae catalysts often results from their highly electropositive nature that increases upon descending group 2.[30] These key features induce the formation of highly reactive d^0 complexes where bonding is essentially governed by electrostatic factors. Some discernible trends have emerged in Ae-mediated catalysis, as recently summarised by Hill and co-workers.[4] Reaction rates usually increase in the order Ca < Sr < Ba, although a few cases exist where the opposite trend is observed, most notably for the cyclohydroamination of aminoalkenes.[6,31,32] Alkaline-earth catalysis usually follows one of the two main operative mechanisms: σ-bond metathesis that involve either protic or hydridic hydrogen atoms, and insertion of a polarised $C^{(\delta+)}=E^{(\delta-)}$ bond (E = C, N, O) into a $Ae^{(\delta'+)}–X^{(\delta'-)}$ bond (X = C, H). Yet, a different catalytic manifold was recently described for the Ae-promoted formation of silazanes upon dehydrocoupling of amines and hydrosilanes. The kinetically prohibited σ-bond metathesis was discarded in favour of a much more facile stepwise process that involves formation of a transient hypervalent hydrosilicate and rate-limiting hydride transfer to the metal (Scheme 1).[27,33,34]

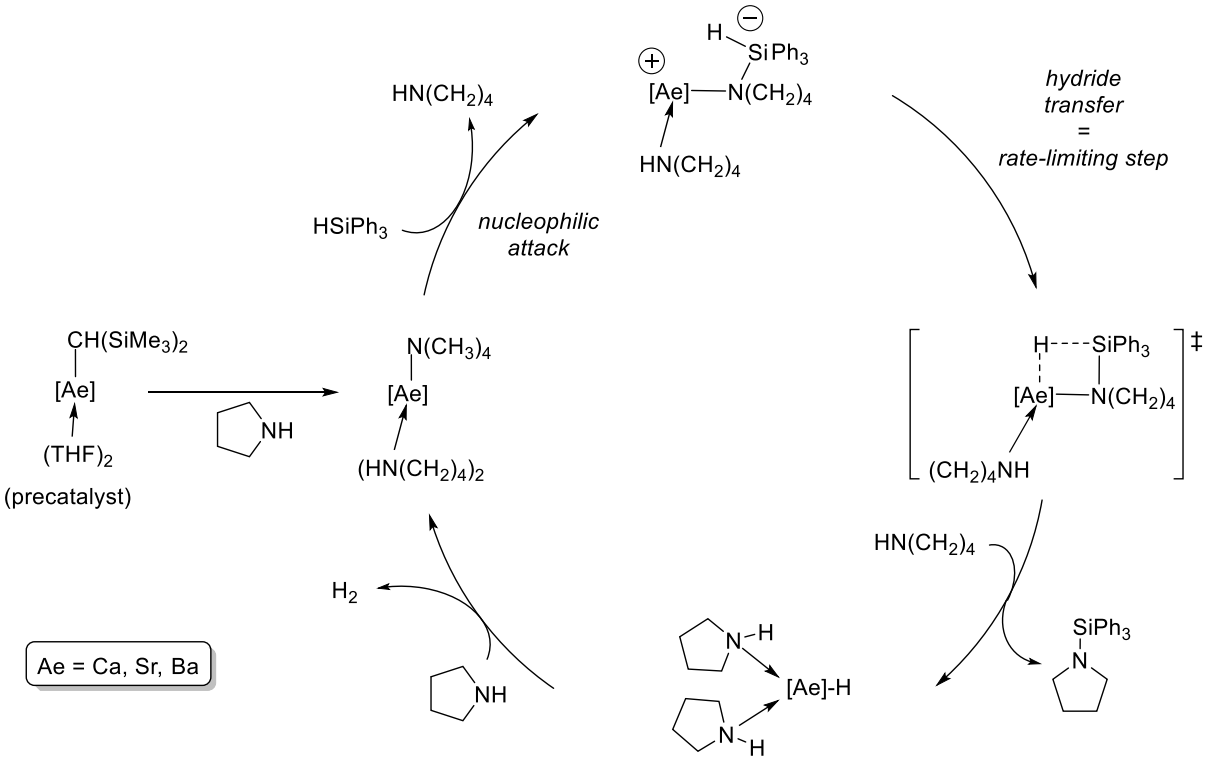

Scheme 1. Stepwise mechanism for alkaline-earth-catalysed dehydrocoupling of amines and hydrosilanes.[27,34]

 10.1002/chem.201904933

We have recently communicated on low coordinate barium boryloxides such as the dimeric $[Ba\{\mu^2\text{-}N(SiMe_3)_2\}(OB\{CH(SiMe_3)_2\}_2)]_2$ (**1₂**) and the monomeric $[Ba(OB\{CH(SiMe_3)_2\}_2)_2]$ (**2**).[29] These complexes catalyse the dehydrocoupling of $\{(Me_3Si)_2CH\}_2BOH$ and hydrosilanes $HSiR_3$ to competently generate borasiloxanes $\{(Me_3Si)_2CH\}_2BOSiR_3$. Besides, barium precatalysts proved superior to their strontium and, even more so, calcium analogues. Borasiloxanes, which contain [B–O–Si] sequences, can be used to produce borosilicates,[35] heat and chemical resistant polymers, and polymer sensors.[36] Traditional synthetic routes typically involve the condensation of various boron- and silicon-based reagents, but suffer from low atom-efficiency and selectivity, and commonly entail the release of toxic or corrosive wastes.[37-39] Prior to our communication, a handful of catalysed processes relying on late transition metal complexes,[40-43] $Sc(OTf)_3$[44] or $Mo(CO)_6$ [45] had been shown to yield borasiloxanes upon coupling of silanols or hydrosilanes with hydroboranes, diboranes, boraxanes, allylborane or vinylboronates. In a reversed and complementary methodology to borinic acids-hydrosilanes dehydrocoupling, silanols and pinacol- and catecholborane can also be coupled in the absence of specific catalyst.[44,46-47] The known processes for the production of borasiloxanes are summarised in Scheme 2.

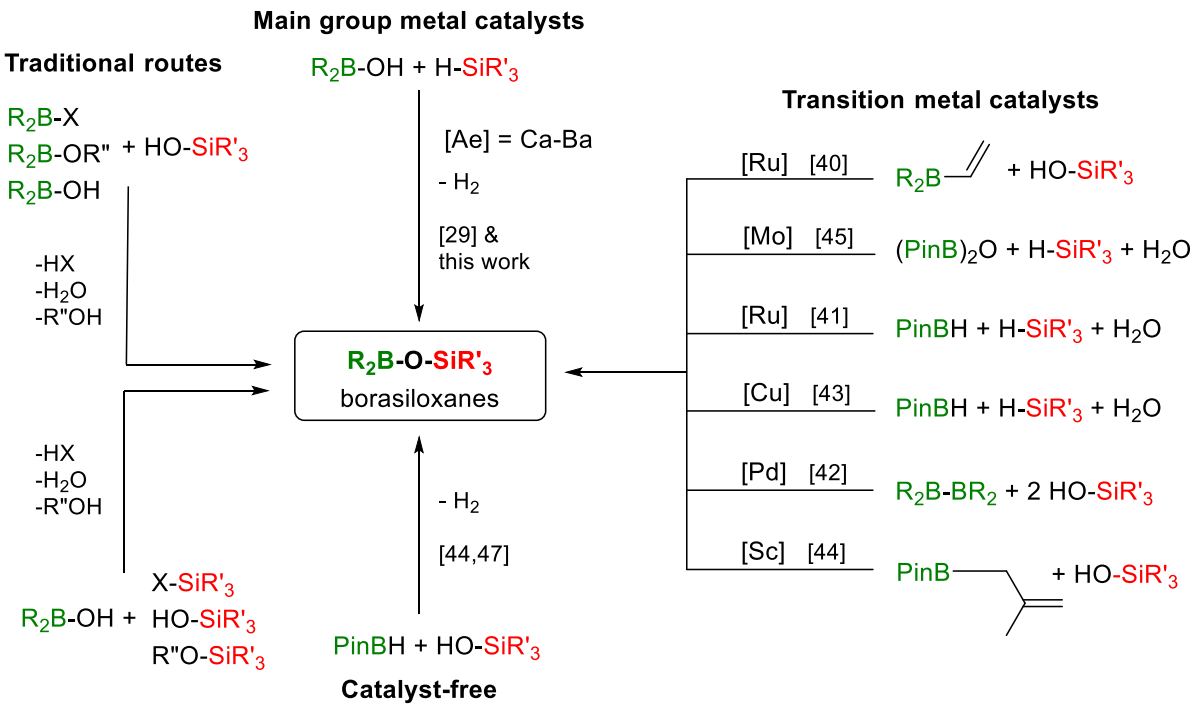

Scheme 2. Summary of synthetic methods for the production of borasiloxanes (Pin = pinacol).

As a continuation of our initial report, we present here the synthesis of new barium boryloxides, and a combined experimental and theoretical (DFT) investigation on the mechanism of the barium-catalysed dehydrocoupling of borinic acids and hydrosilanes. In particular, taken collectively, the data are consistent with a unique modus operandi that involves a dinuclear catalytically active species.

 10.1002/chem.201904933

Results and Discussion

Synthesis and characterisation of barium complexes

We reported in our initial communication that the dimer $[Ba\{\mu^2\text{-}N(SiMe_3)_2\}(OB\{CH(SiMe_3)_2\}_2)]_2$ (**1₂**) could be obtained upon equimolar reaction of $[Ba\{N(SiMe_3)_2\}_2.thf_2]$ and $\{(Me_3Si)_2CH\}_2BOH$, and that further reaction of **1₂** with two equiv of $\{(Me_3Si)_2CH\}_2BOH$ in petroleum ether afforded the monometallic, $[Ba(OB\{CH(SiMe_3)_2\}_2)_2]$ (**2**),[29] the first formally two-coordinate barium complex.

By contrast with the solvent-free **2**, the reaction of **1₂** with two equiv of $\{(Me_3Si)_2CH\}_2BOH$ in toluene affords the adduct $[Ba(OB\{CH(SiMe_3)_2\}_2)_2.C_7H_8]$ [**2**·(tol)] in 90% yield (Scheme 3). This complex can also be synthesised in 75-80% yield from $[Ba\{N(SiMe_3)_2\}_2]_2$ upon treatment with four equiv of $\{(Me_3Si)_2CH\}_2BOH$ in toluene. Diagnostic NMR data in [D₆]benzene for **2**·(tol) include a sharp singlet at δ_{1H} = 0.22 ppm (BC*H*) in the ^{1}H NMR spectrum, and a resonance at δ_{13C} = 21.44 ppm in the $^{13}C\{^1H\}$ spectrum. The ^{11}B NMR spectrum features a single, rather broad singlet at δ_{11B} = 46.13 ppm, i.e. in a region very similar to that for **1₂** (43.67 ppm) and **2** (45.80 ppm). The data in solution in [D₆]benzene also suggest that the toluene molecule is at best loosely bound to or simply dissociated from the Ba^{2+} cation, as its resonances are unsurprisingly identical to those of free toluene in this solvent. Yet, in the solid state, toluene could not be removed from **2**·(tol) upon moderate heating under dynamic vacuum (10^{-2} torr) for several hours. The rather stable coordination of this weak ligand (for d^0 Ae complexes, unable to involve in d-π* back-donation) highlights the very electrophilic character of **2**, in agreement with the presence of intra- and intermolecular agostic Ba···H–C interactions in the molecular solid-state structure of this complex.[29]

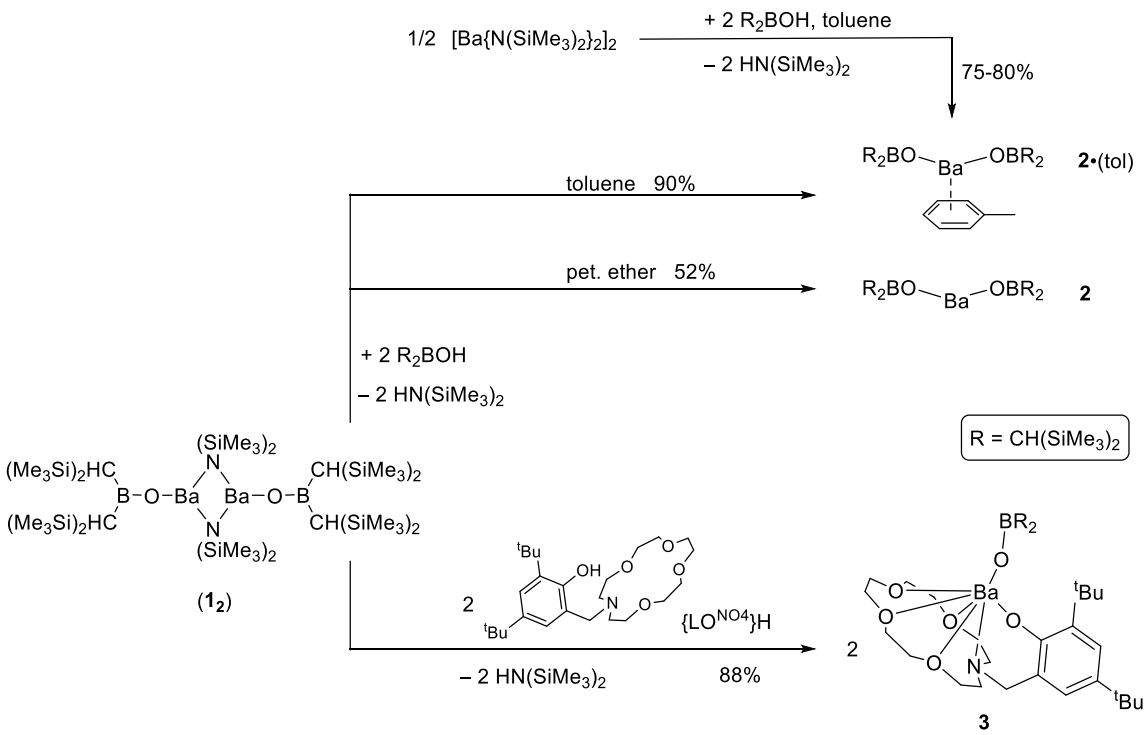

Scheme 3. Synthesis of barium boryloxides.

 10.1002/chem.201904933

Heteroleptic Ae complexes bearing a bulky ancillary ligand usually display better catalytic performances than their ligand-free counterparts.[2-5] We hence sought to prepare such type of precatalyst, and turned for this purpose to a ligand we have used previously. The heteroleptic boryloxo complex [{LO^{NO4}}BaOB{CH(SiMe$_3$)$_2$}$_2$] (**3**), stabilised by the monoanionic aminoetherphenolate {LO^{NO4}}$^-$ that we have utilised to obtain a range of ring-opening polymerisation precatalysts,[5,22] was isolated in 88% yield following the stoichiometric reaction of **1$_2$** with {LO^{NO4}}H (Scheme 3). Complex **3** is poorly soluble in aromatic hydrocarbons. Besides, it is not stable in solution in toluene or benzene at room temperature. NMR data recorded in [D$_6$]benzene show that it decomposes within 15 min through ligand redistribution to give a mixture of **3**, [{LO^{NO4}}$_2$Ba and a species akin to **2**, with concentrations in homoleptic species that increase with time until full ligand shuffling is reached (see SI, Figure S40). For this reason, the reaction time for adequate preparation of solutions of **3** must be kept to 5-10 min. The complex is characterised by a resonance at δ_{11B} = 52.22 ppm in its ^{11}B NMR spectrum, i.e. paradoxically downfield compared to those of **1$_2$**, **2** and **2**·(tol) (δ_{11B} = 43.67, 45.80 and 46.13 ppm).

Single crystals of **2**·(tol) were grown from a saturated toluene solution at –43 °C. The compound is a rare occurrence of three-coordinate monomer, with a toluene molecule coordinated in η^6 fashion (Figure 1). Unusually,[48] the arrangement about Ba1 is trigonal planar (Σ_θ(Ba1) = 360.0°), using the centroid of the aromatic ring (Ba1–Ct = 3.1778(5) Å) to represent the coordinated toluene. The Ba1–C interatomic distances in **2**·(tol), within 3.341(2)-3.5152(25) Å, compare well to those in known toluene adducts.[49-50]

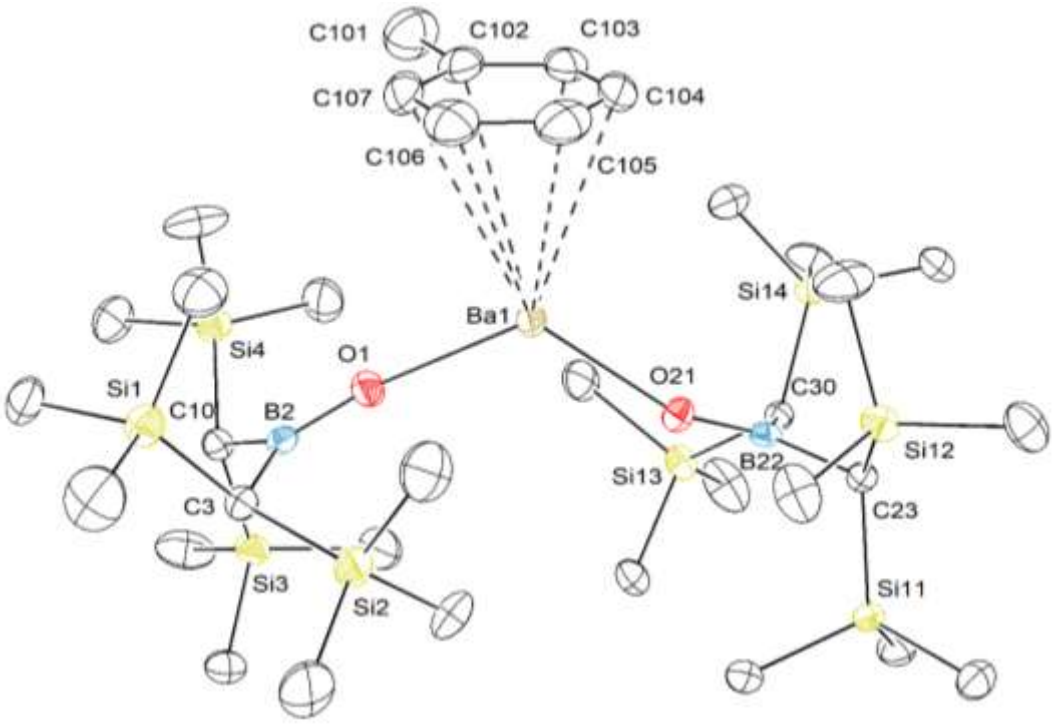

Figure 1. ORTEP view of the molecular structure of [Ba(OB{CH(SiMe$_3$)$_2$}$_2$)$_2$.C$_7$H$_8$] (**2**·(tol)). H atoms omitted for clarity. Ellipsoids at the 50% probability level. Selected interatomic distances (Å) and angles (°): Ba1–O1 = 2.3852(14), Ba1–O21 = 2.3922(13), Ba1–C102 = 3.5093(22), Ba1–C103 = 3.409(2), Ba1–C104 = 3.341(2), Ba1-

 10.1002/chem.201904933

C105 = 3.356(2), Ba1–C106 = 3.4426(26), Ba1–C107 = 3.5152(25), Ba–centroid = 3.1778(5), O1–B2 = 1.334(3), O21–B22 = 1.334(3); O1–Ba1–O21 = 121.35(5), O1–Ba1–centroid = 109.156(38), O21–Ba1–centroid = 129.489(35), O1–B2–C10 = 121.44(19), O1–B2–C3 = 120.06(19), C10–B2–C3 = 118.49(17), O21–B22–C30 = 120.70(18), O21–B22–C23 = 122.46(18), C30–B22–C23 = 116.84(16), B2–O1–Ba1 = 167.12(14), B22–O21–Ba1 = 158.61(13).

The O–Ba–O angle in **2**·(tol) (121.35(5) °) is substantially lower than in the solvent free **2** (130.59(6) °), which is thought to reflect the steric constraint imposed by the presence of toluene. However, the Ba–O distances are very similar in the two complexes (2.3852(14) and 2.3922(13) Å in **2**·(tol), 2.3842(16) and 2.4098(16) Å in **2**). The two boron atoms B2 and B22 are also in a trigonal planar geometry ($\Sigma_\theta(B_i)$ = 360.0°).

The metallic centre is seven-coordinate in the heteroleptic complex **3** (Figure 2). The Ba–$O_{phenolate}$ interatomic distance in **3** (Ba1–O51 = 2.495(2) Å) matches that in the amido congener [{LO^{NO4}}BaN($SiMe_2H$)$_2$] (2.4798(14) Å),[51] and the two complexes are on the whole structurally comparable. The π contribution to the O21–Ba1 and O21–B22 bonds is confirmed by the very wide B22–O21–Ba1 angle of 174.00(2) Å. The Ba1–O21 distance between the metal and $O_{boryloxide}$ of 2.458(2) Å is longer than those in **2** and **2**·(tol). This echoes the greater electronic density on barium and weaker Ba–$O_{boryloxide}$ bond in **3** owing to coordination of the heteroatoms in the aza-crown-ether tether.

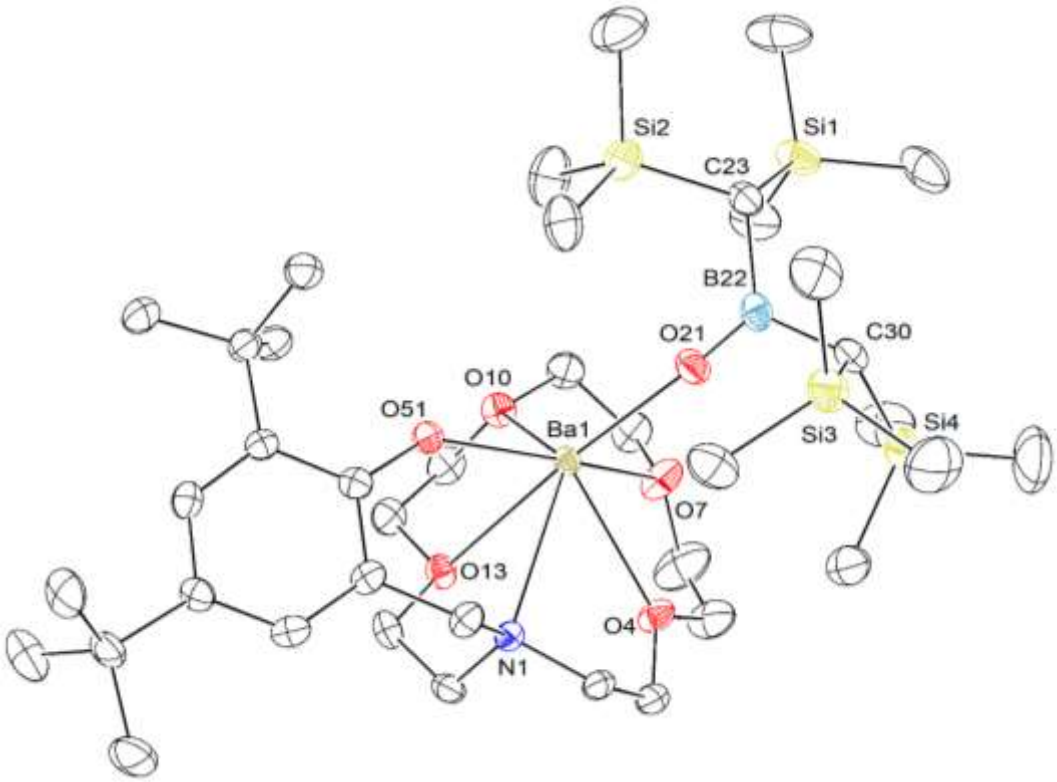

Figure 2. ORTEP view of the molecular structure of [{LO^{NO4}}BaOB{CH($SiMe_3$)$_2$}$_2$] (**3**). Non-interacting toluene molecule not represented. H atoms omitted for clarity. Selected interatomic distances (Å) and angles (°): Ba1–O4 = 2.769(2), Ba1–O7 = 2.921(2), Ba1–O10 = 2.759(2), Ba1–O13 = 2.940(2), Ba1–O21 = 2.458(2), Ba1–O51 = 2.495(2), Ba1–N1 = 2.886(2); B22–O21–Ba1 = 174.00(2), O21–B22–C23 = 120.90(3), O21–B22–C30 = 120.80(3), C23–B22–C30 = 118.30(3).

 10.1002/chem.201904933

Dehydrocoupling catalysis

The boryloxides **1₂**, **2** and **2**·(tol), as well as the simple amido parent precursors $[Ba\{N(SiMe_3)_2\}_2]_2$ and $[Ba\{N(SiMe_3)_2\}_2.(thf)_2]$ (≡ **4₂** and **4**·$(thf)_2$, respectively),[52] catalyse the dehydrocoupling of borinic acids and hydrosilanes (Scheme 4). Due to its chronic instability in solution, **3** was not suited to this purpose.

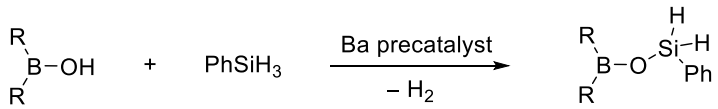

Scheme 4. Barium-mediated dehydrocoupling of borinic acids and hydrosilanes.

The coupling of $\{(Me_3Si)_2CH\}_2BOH$) with $PhSiH_3$ was used as benchmark reaction. As communicated earlier,[29] the coupling of 50-100 equiv of both substrates (1:1) vs Ba occurred readily at 60 °C, generating $PhSi(H)_2OB\{CH(SiMe_3)_2\}_2$ in quantitative yields. The main conclusions of the initial investigation, for which the easily accessed **4**·$(thf)_2$ precatalyst was used, can be summarised as follows: (i) the reactions are chemoselective, as for instance only one coupling occurs with $PhSiH_3$ even with excess $\{(Me_3Si)_2CH\}_2BOH$, (ii) reaction rates increased according to Ca < Sr < Ba, (iii) **4₂** and **4**·$(thf)_2$ were the most efficient precatalysts, (iv) the kinetic rate law using the mononuclear **4**·$(thf)_2$ showed first order dependence on $[PhSiH_3]$, second order on [**4**·$(thf)_2$] and zeroth order on $[\{(Me_3Si)_2CH\}_2BOH]$, with $\Delta H^{\ddagger}$ = 9.1(2) kcal mol^{-1}, $\Delta S^{\ddagger}$ = –24.2(8) cal mol^{-1} K^{-1} and $\Delta G^{\ddagger}$ = 16.3(5) kcal mol^{-1} at 25 °C, (v) isolated data points suggested that reaction rates increased (resp. decreased) upon introduction of electron-withdrawing (resp. electron-donating) groups in *para* position in *p*-X-$C_6H_4SiH_3$ substrates, and (vi) substrate scope could be extended from aryl to alkoxy- and alkylsilanes, with the order of reactivity $(^iPrO)_3SiH$ < $^nBuSiH_3$ < $PhSiH_3$. However, the substrate scope regarding the borinic acid was at the time not probed, while kinetic data were incomplete. Besides, the second order dependence on [Ba] was unusual, and no mechanism could be proposed.

By comparison with the fairly reactive $\{(Me_3Si)_2CH\}_2BOH$, other borinic acids were less effective in the dehydrocoupling with $PhSiH_3$ catalysed by **4**·$(thf)_2$. Discriminating experiments were conducted in this aim (Scheme 5). They showed that whereas 75% of 100 equiv of $\{(Me_3Si)_2CH\}_2BOH$ and $PhSiH_3$ (1:1) were converted to $PhSi(H)_2OBR_2$ in 8 h at 60 °C, reactions with the aromatic-substituted borinic acids $(Mes)_2BOH$ (Mes = mesityl), $(2,4,6\text{-}(CF_3)_3\text{-}C_6H_2)_2BOH$ and $(2,4,6\text{-}^iPr_3\text{-}C_6H_2)_2BOH$ required more forcing conditions ($[SiH]_0/[BOH]_0/[Ba]_0$ = 10:10:1, 24 h, 60 °C), and only reached very moderate, if any, conversion to the desired product (resp. 0, 30 and 37%). In particular, with the least bulky $(Mes)_2BOH$, catalysis is irremediably plagued by concurrent spontaneous dehydration upon formation of the catalytically inert $Mes_2B–O–BMes_2$, which could be identified spectroscopically. Clearly, this dehydrocoupling catalysis requires careful consideration of steric factors to be successful, and seems so far to be restricted to these sterically protected borinic acids which do not spontaneously form B-O-B containing species and release H_2O noxious to the catalyst. The reasons behind the greater reactivity of

$\{(Me_3Si)_2CH\}_2BOH$ with respect to $(2,4,6\text{-}^iPr_3\text{-}C_6H_2)_2BOH$ and $(2,4,6\text{-}(CF_3)_3\text{-}C_6H_2)_2BOH$ are not clear at this stage. The nucleophilic character of the metal-bound oxygen atom in the Ba-O-B fragment plays a key role in the proposed catalytic mechanism (see below). One might hypothesise that the observed reactivity mirrors the greater nucleophilicity of the O atoms in $\{(Me_3Si)_2CH\}_2BOH/\{(Me_3Si)_2CH\}_2BO^-$ than in the aromatic congeners. It may also be that the boryloxides $(2,4,6\text{-}^iPr_3\text{-}C_6H_2)_2BO^-$ and $(2,4,6\text{-}(CF_3)_3\text{-}C_6H_2)_2BO^-$, because they can give rise to Ba···F–C and Ba···Cπ interactions, generate more stable and hence less reactive barium species than $\{(Me_3Si)_2CH\}_2BO^-$. Finally, we note that these barium-mediated reactions are chemoselective. They lead solely to the production of the products of monocoupling $PhSi(H)_2OB\{CH(SiMe_3)_2\}_2$, $PhSi(H)_2OB(2,4,6\text{-}^iPr_3\text{-}C_6H_2)_2$ and $PhSi(H)_2OB(2,4,6\text{-}(CF_3)_3\text{-}C_6H_2)_2$, without detectable formation of tertiary or quaternary silanes.

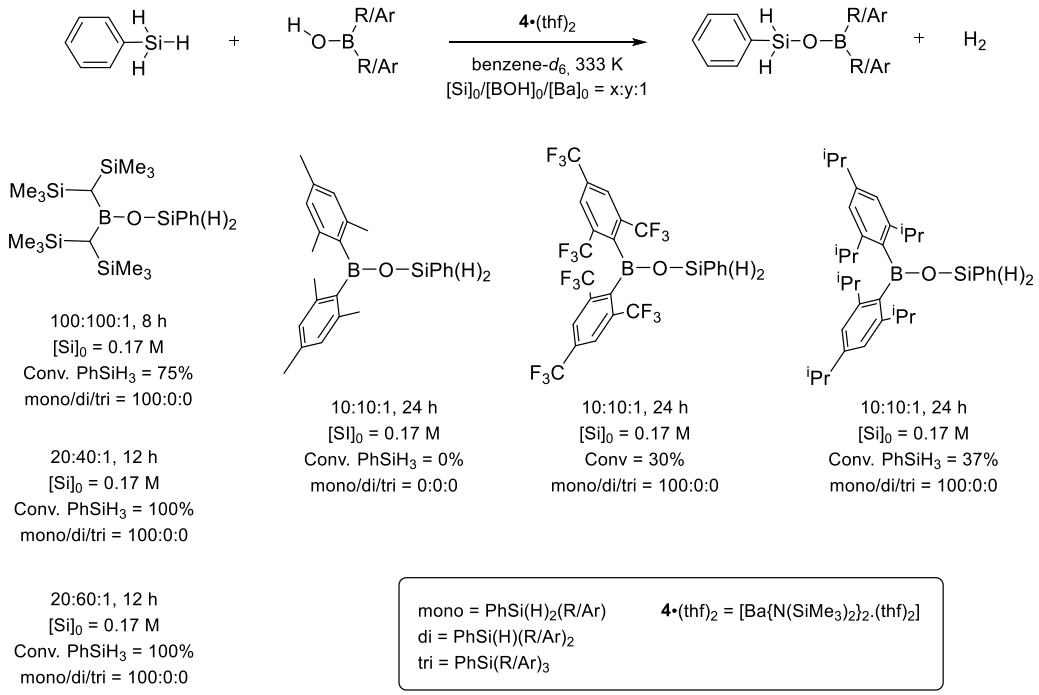

Scheme 5. Dehydrocoupling of $PhSiH_3$ and various borinic acids mediated by **4**·$(thf)_2$.

Additional kinetic analysis was performed for the benchmark coupling of $PhSiH_3$ and $\{(Me_3Si)_2CH\}_2BOH$ in order to provide complementary data to our initial investigation and improve our general understanding of the catalytic manifold. We started by gauging the respective efficiencies of **4**·$(thf)_2$ and $\mathbf{4_2}$, and showed that the latter is clearly superior (and, in fact, the most effective precatalyst in this catalysis). An apparent rate constant (k_{app}) of $3.12(4)\cdot10^{-4}$ s^{-1} was estimated from the semi-logarithmic plot of substrate conversion vs. time for the coupling of $\{(Me_3Si)_2CH\}_2BOH$ and $PhSiH_3$ (1:1) with a loading in $\mathbf{4_2}$ of 0.125 mol-%; the corresponding optimised TOF (at 15% conversion) was 456 mol_{subs} mol_{Ba}^{-1} h^{-1}. By comparison, for the solvated **4**·$(thf)_2$, $k_{app} = 3.40(3)\cdot10^{-4}$ s^{-1} was determined for a higher precatalyst loading (1.5 mol-%), corresponding to an overall activity lowered by about an order of magnitude, TOF = 71 mol_{subs} mol_{Ba}^{-1} h^{-1} also at 15% conversion. In fact, $\mathbf{4_2}$ was often too fast

 10.1002/chem.201904933

for convenient and reliable kinetic monitoring by NMR spectroscopy at 25 °C, and we found **4**·$(thf)_2$ was better suited for this purpose.

A full Hammett analysis was carried out (see SI, S42-S43) to assess more accurately the influence of electron-withdrawing/donating groups in *para*-substituted arylsilanes *p*-X-C_6H_4-SiH_3 in the coupling with $\{(Me_3Si)_2CH\}_2BOH$ catalysed by **4**·$(thf)_2$ (T = 40 °C, $[Si]_0/[BOH]_0$ = 1:1, $[Ba]_0$ = 0.85-4.23 mM in $[D_6]$benzene). Rate constants k_X of 31.48(21), 40.10(19), 54.80(15) and 64.80(26) s^{-1} M^{-2} were determined for X = OMe, Me, H and F, respectively. Reaction rates hence clearly increased by introducing electron-withdrawing substituents. The plot of $\ln(k_X/k_H)$ vs $\sigma_P(X)$ gave a largely positive slope, ρ = 2.03(9), compatible with a mechanism involving the accumulation of a negative charge on the silicon atom in the rate-determining step of the catalytic cycle.

We surmised that the partial kinetic order of 2 in [precatalyst] determined for the coupling of $\{(Me_3Si)_2CH\}_2BOH$ and $PhSiH_3$ catalysed by the *mononuclear* **4**·$(thf)_2$ indicated the reaction traversed an associated dinuclear transition state; this was compatible with the large negative entropy of activation, $\Delta S^{\ddagger}$ = –24.2(8) cal mol^{-1} K^{-1}.[29] This assumption proved justified since, under otherwise identical conditions, the reaction catalysed by the *dinuclear* precatalyst $[Ba\{\mu^2\text{-}N(SiMe_3)_2\}(OB\{CH(SiMe_3)_2\}_2)]_2$ (**1₂**) unambiguously exhibited first-order kinetics in [dinuclear precatalyst], see Figure S44 in SI. Hence, the rate law for these barium-promoted dehydrocouplings can be written as in equation (1),

$$Rate = -d[PhSiH_3]/dt = k.[\text{Ba precatalyst}]^{2-x}.[PhSiH_3] \quad (1)$$

where x = 1 for a dinuclear Ba precatalyst as in $\mathbf{1_2}$ or $\mathbf{4_2}$ and, conversely, x = 0 for a mononuclear complex as in **4**·$(thf)_2$.

Computational analysis

The operative mechanism for the dehydrocoupling reaction of borinic acids with hydrosilanes catalysed by barium boryloxides was investigated by DFT calculations, in light of the experimental kinetic analysis. Structure optimisation and evaluation of conceivable mechanistic pathways were carried out with the aid of a reliable DFT methodology (single point energy calculations on the BP86-D3 geometries using the PBE0-D3 functional and the triple-ζ TZVP basis set for main group atoms, see SI). All computational studies were carried out with $\{(Me_3Si)_2CH\}_2BOH$ as borinic acid and $PhSiH_3$ as hydrosilane. THF-free (pre)catalysts **4**, $[Ba\{\mu^2\text{-}N(SiMe_3)_2\}(OB\{CH(SiMe_3)_2\}_2)]_2$ ($\mathbf{1_2}$) and $Ba\{OB(CH(SiMe_3)_2)_2\}_2$ (**2**) were considered.

We first focused on the possible catalytically active species that can be formed under reaction conditions. The system involving the putative *monomeric* **4** was set as zero point energy in Scheme 6. Both monomeric and dimeric barium species were evaluated. In the case of monomeric species, the replacement of one amide on barium by a boryloxide leads, via the adduct **4**·($\{(Me_3Si)_2CH\}_2BOH$), to the formation of the mixed species $[Ba\{N(SiMe_3)_2\}OB\{CH(SiMe_3)_2\}]$ (aka **1**, the monomeric unit in synthetically isolated $\mathbf{1_2}$) with an energy gain of 15.4 kcal mol^{-1}. From this point, further substitution of

10.1002/chem.201904933

the remaining amide by another boryloxide leading to **2** is favoured by another 9.3 kcal mol^{-1}. Finally, saturation of the coordination sphere by an additional $\{(Me_3Si)_2CH\}_2BOH$ yields $[Ba(OB\{CH(SiMe_3)_2\}_2)_2\cdot\{(Me_3Si)_2CH\}_2BOH]$ [**2**·($\{(Me_3Si)_2CH\}_2BOH$)], a species 33.0 kcal mol^{-1} more stable than **4**. Coordination of a second borinic acid onto **2**·($\{(Me_3Si)_2CH\}_2BOH$) is precluded by the steric constraint imposed by the bulky ligands.

Regarding dimeric species, four structures have been considered, namely $\mathbf{1_2}$, $\mathbf{2_2}$, $\mathbf{4_2}$ and $\mathbf{2_2}'$. Dimers $\mathbf{1_2}$ and $\mathbf{4_2}$ present a three-coordinate barium with $N(SiMe_3)_2$ groups bridging the two metals and have terminal boryloxide or amide groups, respectively. As already highlighted for monomeric species, boryloxide ligands stabilise the metal environment to a greater extent with respect to amides, so that $\mathbf{1_2}$ is 31.5 kcal mol^{-1} more stable than $\mathbf{4_2}$. As for **2**, in agreement with the X-ray analysis,[29] we localised species $\mathbf{2_2}$, consisting in two $Ba\{OB(CH(SiMe_3)_2)_2\}_2$ units interacting only by multiple intermolecular agostic Ba···H–C interactions, with long Ba–O_1 distances (4.89 Å). Alternatively, the two **2** units can be bridged by boryloxides with short Ba–O_1 distances of 2.62 Å ($\mathbf{2_2}'$ in Scheme 6). The former species, $\mathbf{2_2}$, is 7.0 kcal mol^{-1} more stable than $\mathbf{2_2}'$, and is therefore very largely preponderant. Overall, the energy scenario emerging from Scheme 6 strongly suggests that any Ba-amide or Ba-boryloxide precatalyst is very likely to dimerise to $\mathbf{2_2}$ under reaction conditions. As a consequence, this complex is referred to as the zero-point energy for the mechanistic pathway depicted in Scheme 7.

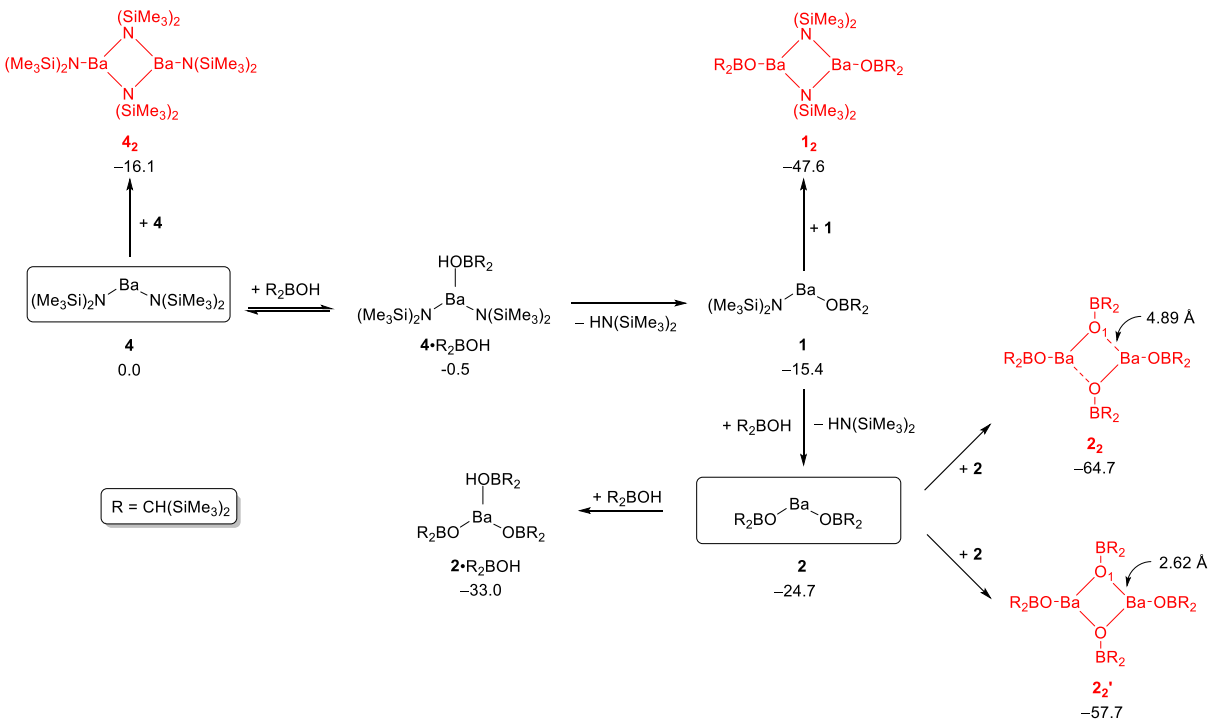

Scheme 6. Monomeric (black) and dimeric (red) barium species. Free energies (in kcal mol^{-1}) are given in C_6H_6.

The catalytic cycle (Scheme 7) starts with the nucleophilic attack of one of the oxygens of $\mathbf{2_2}$ onto $PhSiH_3$, via transition state TS($\mathbf{2_2}$-**B**) with an energy barrier of 19.8 kcal mol^{-1}. The following transient

 10.1002/chem.201904933

intermediate **B** presents a negatively charged five-coordinate silicate and evolves easily (barrier for **B→C** step = 3.6 kcal mol^{-1}) to the more stable intermediate **C** through replacement of the bridging oxygen by the Si-H moiety. This step is required to facilitate the following hydrogen transfer (**C→D**) affording the bridged barium hydride **D** with release of the coupled product $PhSi(H)_2O\{CH(SiMe_3)_2\}_2$. All attempts to either localise a transition state for hydrogen transfer starting from **B** or compute a viable reaction pathway for the direct conversion of $\mathbf{2_2}$ + $PhSiH_3$ into **D** via σ-bond metathesis involving Ba–O, Ba–H, Si–O and Si–H bonds, failed due to the steric congestion imposed by the bulky boryloxides.

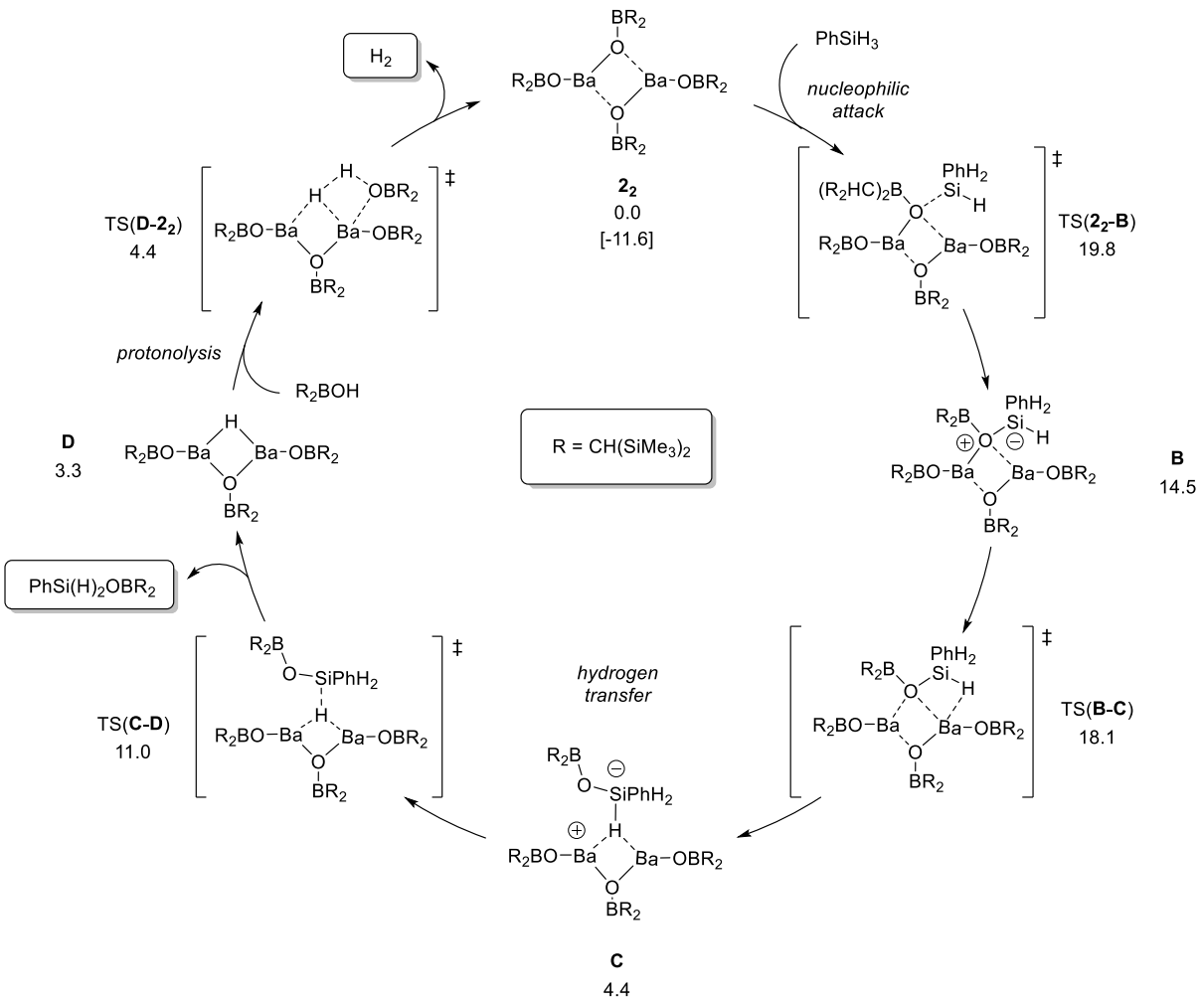

Scheme 7. Dimeric pathway for the dehydrocoupling of $\{(Me_3Si)_2CH\}_2BOH$ with $PhSiH_3$ by a Ba-OBR_2 catalyst. Free energies (in kcal mol^{-1}) are given in C_6H_6. The number in brackets takes into account the thermodynamic of the dehydrocoupling.

The **C→D** step advances very easily, with a relatively low energy barrier of only 6.6 kcal mol^{-1} with respect to **C**. Reaction of **D** with an additional $\{(Me_3Si)_2CH\}_2BOH$ that coordinates to barium and promotes the releasing of H_2 regenerates the starting catalyst without a real barrier (only 1.1 kcal mol^{-1} with respect to **D**) through transition state TS(**D-2₂**). Overall, the proposed pathway is hence kinetically ruled by the initial nucleophilic attack of barium boryloxide to the incoming hydrosilane; the computed energy barrier $\Delta G^{\ddagger}$ of 19.8 kcal mol^{-1} is reasonably close to the experimental value (16.3(5) kcal mol^{-}

 10.1002/chem.201904933

[1]), and the thermochemistry of the reaction between $PhSiH_3$ and $\{(Me_3Si)_2CH\}_2BOH$ that affords $PhSi(H)_2OB\{CH(SiMe_3)_2\}_2$ and H_2 is estimated to –11.6 kcal mol^{-1} at this level of theory. On the basis of this computational insight, we infer that the generation of borasiloxanes in the presence of barium precatalysts proceeds through a stepwise mechanism with dinuclear catalytically active species. The experimentally observed partial kinetic orders in [Ba] of two for the monometallic **1**.(thf)$_2$ and one for the bimetallic $\mathbf{1_2}$ fully agree with the presence of two barium centres along all the reaction pathway as delineated by these DFT computations.

An alternative pathway involving instead a monomeric barium moiety was investigated in an attempt to gauge the role of the second barium unit in the dimeric mechanism. The most stable monomeric adduct **2**·($\{(Me_3Si)_2CH\}_2BOH$) (see Scheme 6) was set as zero-point energy reference in Scheme 8. This reaction pathway starts with nucleophilic attack of an oxygen atom onto the silicon atom of incoming $PhSiH_3$, leading to the high energy silicate intermediate **E**.

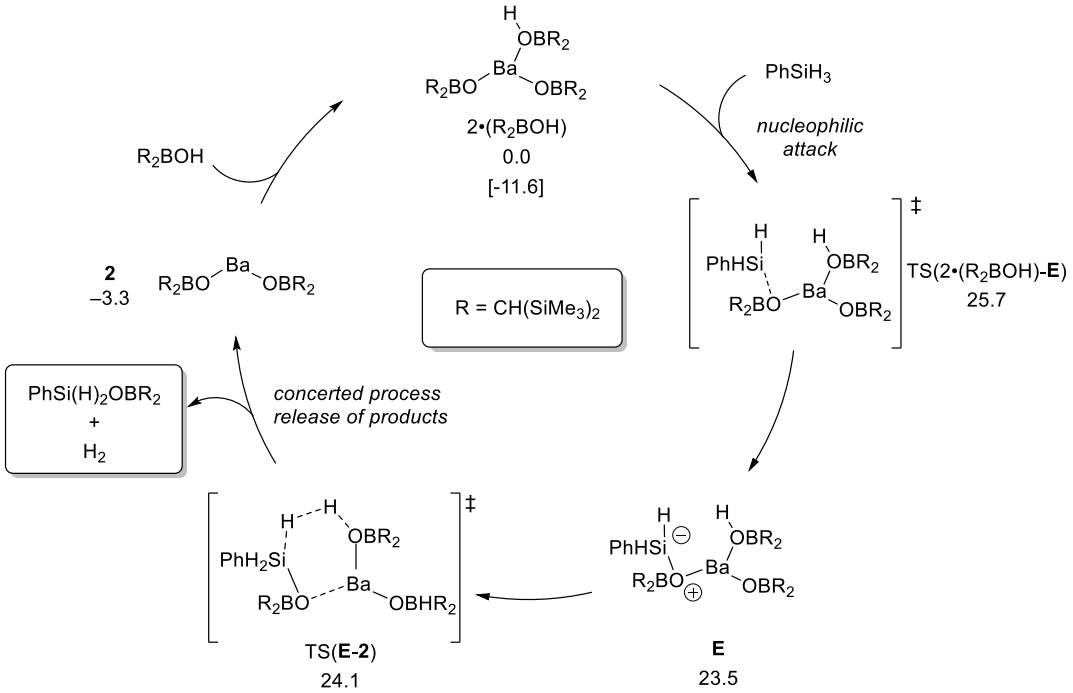

Scheme 8. Alternative monomeric pathway for dehydrocoupling reaction of borinic acid with $PhSiH_3$ by barium boryloxide catalyst. Free energies (in kcal/mol) are given in C_6H_6. The number in brackets takes into account the thermodynamics of the dehydrocoupling; hence, the energy released upon regeneration of **2**·($\{(Me_3Si)_2CH\}_2BOH$) from **2** will be on the whole –8.3 kcal mol^{-1}, as found in Scheme 6.

From there, the energetically favoured mechanism consists in the formation of H_2 upon coupling of the Si–H and the O–H hydrogens with release of the product $PhSi(H)_2OB\{CH(SiMe_3)_2\}_2$, and transient formation of **2**. Coordination of an external $\{(Me_3Si)_2CH\}_2BOH$ regenerates the starting species. Overall, this manifold imposes to overcome an energy barrier of 25.7 kcal mol^{-1}; this is 5.9 kcal mol^{-1} greater than for the rate determining transition state in the bimetallic pathway (Scheme 7), and the likelihood of this scenario is therefore soundly ruled out. In addition, the monomeric mechanism is also disfavoured due to the instability of its active species, **2**·($\{(Me_3Si)_2CH\}_2BOH$), relative to $\mathbf{2_2}$ (Scheme

6) that is operating in the dimeric mechanism. One should note that the unfavourable monometallic pathway delineated here differs significantly from that established for the barium-catalysed formation of silazanes by coupling of amines and hydrosilanes,[27,34] and in which the prevalent route involves a monomeric four-coordinate barium pyrrolide. As discussed above for **2**·({$(Me_3Si)_2CH\}_2BOH$), coordination of a fourth bulky ligand $\{(Me_3Si)_2CH\}_2BOH$ to the already sterically congested Ba-boryloxides is prohibited. In addition, unlike Ba-pyrrolide NH/HSi dehydrocoupling catalysts for which it was energetically accessible, the prevailing mechanism with monomeric Ba-boryloxide does not involve H-transfer and formation of a Ba-hydride. Instead, cleavage of the Si–H and H–O bonds is synchronous, and leads to H–H bond formation in a concerted event. Finally, it is noteworthy that within the most favourable dimeric pathway, cooperation between the Ba atoms stabilises the Ba-hydride species (**D** in Scheme 7), allowing easier H-transfer and product release.

Concluding remarks

The mechanism of the barium-catalysed dehydrocoupling of borinic acids and hydrosilanes has been delineated by combination of experimental and computational methods. The kinetic rate law was established for these kinetically facile reactions, using the dehydrocoupling of $PhSiH_3$ and $\{(Me_3Si)_2CH\}_2BOH$ as a benchmark reaction. It shows that the dependence in precatalyst concentration varies with the nuclearity of the precatalyst, and overall highlights an operative mechanism that evolves through a highly organised dinuclear transition state in the rate-determining step. This is consistent with the activation parameters, in particular the large entropy of activation, $\Delta S^{\ddagger} = -24.2(8)$ cal mol^{-1} K^{-1}. DFT computations confirm that a mechanistic pathway involving a monometallic pathway is both kinetically and thermodynamically disfavoured over a stepwise mechanism involving bimetallic species. In this prevalent pathway, the catalytically active species is the bis boryloxide $[Ba(OB\{CH(SiMe_3)_2\}_2)_2]_2$. The rate-determining step consists of the nucleophilic attack of a metal-bound oxygen onto the incoming hydrosilane, hence generating a pentavalent hydrosilicate; hydride transfer from this silicate onto the metal is authorised by the presence of a dinuclear species. A putative mechanism involving direct σ-bond metathesis, as most commonly encountered in catalysis mediated by oxophilic elements and in particular alkaline earth, is also energetically unfavourable.

A range of alkaline-earth compounds can catalyse these couplings, but overall barium ones are by far the most competent (Ca < Sr < Ba). We have prepared a range of various Ba-boryloxide precatalysts that display good performances, but $[Ba\{N(SiMe_3)_2\}_2.(thf)_2]$ and even more so $[Ba\{N(SiMe_3)_2\}_2]_2$ are equally, if not more, efficient. These simple amides should be the preferred choice of precatalysts, since they are easier to prepare. An advantage of these reactions is that they are chemoselective. Hence, the reaction of $PhSiH_3$ with a borinic acid R_2BOH, even used in excess, will cleanly generate a monocoupling dihydrosilane $PhSi(H)_2OBR_2$ that may be further used or functionalised thanks to the presence of the remaining two Si-H moieties.

The synthesis of an heteroleptic boryloxide/aminoether-phenolate [{LO^{NO4}}BaOB{$CH(SiMe_3)_2$}$_2$], was successful, although this complex is not sufficiently stable in solution to be implemented in catalysis. Still, the choice of different ancillary ligands can of course be envisaged, for instance bulky β-diketiminates[2-5,54-55] or aminoether-functionalised iminoanilides and amidinates.[56] In line with other Ae-mediated reactions,[2-5] it is possible that the resulting heteroleptic barium complexes will exhibit greater reaction rates than the homoleptic complexes used here. We are now exploring this line of investigations.

The substrate scope is for now somewhat limited to bulky borinic acids, in particular those that are unlikely to generate B-O-B containing species through uncontrolled (thermal) dimerisation and concomitant elimination of water, a phenomenon critically detrimental to the active catalytic species. Future efforts will concentrate on expanding the scope and applicability of these reactions. The synthesis of macromolecules can also be sought, for instance by dehydropolymerisation of an α-hydrosilane-ω-borinic acid, or through polycondensation between a dihydrosilane or α,ω-di(hydrosilane) with a α,ω-di(borinic acid).[23,24]

Supporting Information

Full experimental section; DFT and XRD details; kinetic measurements.

Acknowledgements

L. C., L. F. and Z. Z. thank the King Abdullah University of Science and Technology (KAUST) for supporting this work. For computer time, this research used the resources of the KAUST Super-computing Laboratory (KSL) at KAUST. E. L. C. thank the University of Rennes 1 for a PhD grant.

Conflicts of interest

The authors declare no conflict of interest.

Notes and references

[1] E. Leitao, T. Jurca, I. Manners, *Nat. Chem.* **2013**, *5*, 817.

[2] S. Harder, *Chem. Rev.* **2010**, *110*, 3852.

[3] M. R. Crimmin, M. S. Hill, *Top. Organomet. Chem.* **2013**, *45*, 191.

[4] M. S. Hill, D. J. Liptrot, C. Weetman, *Chem. Soc. Rev.* **2016**, *45*, 972.

[5] Y. Sarazin, J.-F. Carpentier, *Chem. Rec.* **2016**, *16*, 2482.

[6] M. R. Crimmin, I. J. Casely, M. S. Hill, *J. Am. Chem. Soc.* **2005**, *127*, 2042.

[7] F. Buch, J. Brettar, S. Harder, *Angew. Chem. Int. Ed.* **2006**, *45*, 2741.

[8] J. Spielmann, F. Buch, S. Harder, *Angew. Chem. Int. Ed.* **2008**, *47*, 9434.

[9] A. G. M. Barrett, C. Brinkmann, M. R. Crimmin, M. S. Hill, P. Hunt, P. A. Procopiou, *J. Am. Chem. Soc.* **2009**, *131*, 12906.

[10] P. Jochmann, J. P. Davin, T. P. Spaniol, L. Maron, J. Okuda, *Angew. Chem. Int. Ed.* **2012**, *51*, 4452.

[11] B. Liu, T. Roisnel, J.-F. Carpentier, Y. Sarazin, *Angew. Chem. Int. Ed.* **2012**, *51*, 4943.

[12] C. Qi, V. Gandon, D. Lebœuf, *Angew. Chem. Int. Ed.* **2018**, *57*, 14245.

[13] H. Bauer, M. Alonso, C. Fischer, B. Rösch, H. Elsen, S. Harder, *Angew. Chem. Int. Ed.* **2018**, *57*, 15177.

[14] A. S. S. Wilson, C. Dinoi, M. S. Hill, M. F. Mahon, L. Maron, *Angew. Chem. Int. Ed.* **2018**, *57*, 15500.

[15] F. M. Younis, S. Krieck, T. M. Al-Shboul, H. Görls, M. Westerhausen, *Inorg. Chem.* **2016**, *55*, 4676.

[16] H. Bauer, M. Alonso, C. Färber, H. Elsen, J. Pahl, A. Causero, G. Ballmann, F. de Proft, S. Harder, *Nat. Catal.* **2018**, *1*, 40.

[17] J. Spielmann, S. Harder, *Eur. J. Inorg. Chem.* **2008**, 1480.

[18] B. Liu, J.-F. Carpentier, Y. Sarazin, *Chem. Eur. J.* **2012**, *18*, 13259.

[19] M. D. Anker, M. Arrowsmith, P. Bellham, M. S. Hill, G. Kociok-Köhn, D. J. Liptrot, M. F. Mahon, C. Weetman, *Chem. Sci.* **2014**, *5*, 2826.

[20] S. Harder, F. Feil, K. Knoll, *Angew. Chem. Int. Ed.* **2001**, *40*, 4261.

[21] D. F.-J. Piesik, S. Range, S. Harder, *Organometallics* **2008**, *27*, 6178.

[22] Y. Sarazin, B. Liu, T. Roisnel, L. Maron, J.-F. Carpentier, *J. Am. Chem. Soc.* **2011**, *133*, 9069.

[23] C. Bellini, C. Orione, J.-F. Carpentier, Y. Sarazin, *Angew. Chem. Int. Ed.* **2016**, *55*, 3744.

[24] L. J. Morris, G. R. Whittell, J.-C. Eloi, M. F. Mahon, F. Marken, I. Manners, M. S. Hill, *Organometallics* **2019**, *38*, 3629.

[25] J. Spielmann, G. Jansen, H. Bandmann, S. Harder, *Angew. Chem. Int. Ed.* **2008**, *47*, 6290.

[26] M. S. Hill, D. J. Liptrot, D. J. MacDougall, M. F. Mahon, T. P. Robinson, *Chem. Sci.* **2013**, *4*, 4212.

[27] C. Bellini, J.-F. Carpentier, S. Tobisch, Y. Sarazin, *Angew. Chem. Int. Ed.* **2015**, *54*, 7679.

[28] D. J. Liptrot, M. S. Hill, M. F. Mahon, A. S. S. Wilson, *Angew. Chem. Int. Ed.* **2015**, *54*, 13362.

[29] E. Le Coz, V. Dorcet, T. Roisnel, S. Tobisch, J.-F. Carpentier, Y. Sarazin, *Angew. Chem. Int. Ed.* **2018**, *57*, 11747.

[30] Pauling electronegativity: Ca, 1.00; Sr, 0.95; Ba, 0.89. Ionic radius for C.N. = 6: Ca^{2+}, 1.00; Sr^{2+}, 1.18; Ba^{2+}, 1.35.

[31] S. Tobisch, *Chem. Eur. J.* **2015**, *21*, 6765.

[32] M. R. Crimmin, A. G. M. Barrett, M. S. Hill, P. A. Procopiou, *Org. Lett.* **2007**, *9*, 331.

[33] J. F. Dunne, S. R. Neal, J. Engelkemier, A. Ellern, A. D. Sadow, *J. Am. Chem. Soc.* **2011**, *133*, 16782.

[34] C. Bellini, V. Dorcet, J.-F. Carpentier, S. Tobisch, Y. Sarazin, *Chem. Eur. J.* **2016**, *22*, 4564.

[35] R. Pena-Alonso, G. Mariotto, C. Gervais, F. Babonneau, G. D. Soraru, *Chem. Mater.* **2007**, *19*, 5694.

[36] W. Liu, M. Pink, D. Lee, *J. Am. Chem. Soc.* **2009**, *131*, 8703.

[37] D. A. Foucher, A. J. Lough, I. Manners, *Inorg. Chem.* **1992**, *31*, 3034.

[38] K. L. Fujdala, A. G. Oliver, F. J. Hollander, T. D. Tilley, *Inorg. Chem.* **2003**, *42*, 1140.

[39] M. Pascu, A. Ruggi, R. Scopelliti, K. Severin, *Chem. Commun.* **2013**, *49*, 45.

[40] B. Marciniec, J. Walkowiak, *Chem. Commun.* **2008**, 2695.

[41] B. Chatterjee, C. Gunanathan, *Chem. Commun.* **2017**, *53*, 2515.

[42] A. Yoshimura, M. Yoshinaga, H. Yamashita, M. Igarashi, S. Shimada, K. Sato, *Chem. Commun.* **2017**, *53*, 5822.

[43] A. Dhakshinamoorthy, A. M. Asiri, P. Concepcion, H. Garcia, *Chem. Commun.* **2017**, *53*, 9998.

[44] J. Kaźmierczak, K. Kuciński, H. Stachowiak, G. Hreczycho, *Chem. Eur. J.* **2018**, *24*, 2509.

[45] M. Ito, M. Itazaki, H. Nakazawa, *J. Am. Chem. Soc.* **2014**, *136*, 6183.

[46] R. A. Metcalfe, D. I. Kreller, J. Tian, H. Kim, N. J. Taylor, J. F. Corrigan, S. Collins, *Organometallics* **2002**, *21*, 1719.

[47] K. Kuciński, G. Hreczycho, *ChemSusChem* **2017**, *10*, 4695.

[48] See for instance the similar geometry in the bariate $[K(IPr)_2][Ba\{N(SiMe_3)_2\}_3]$, where IPr = 1,3-bis(2,6-di-isopropylphenyl)-imidazol-2-ylidene: M. S. Hill, G. Kociok-Köhn, D. J. MacDougall, *Inorg. Chem.* **2011**, *50*, 5234.

[49] M. Westerhausen, M. Krofta, N. Wiberg, H. Noth, A. Pfitzner, *Z. Naturforsch., B: Chem. Sci.* **1998**, *1489*, 53.

[50] O. Michel, S. König, K. W. Törnroos, C. Maichle-Mössmer, R. Anwander, *Chem. Eur. J.* **2011**, *17*, 11857.

[51] Y. Sarazin, D. Roşca, V. Poirier, T. Roisnel, A. Silvestru, L. Maron, J.-F. Carpentier, *Organometallics* **2010**, *29*, 6569.

[52] M. Westerhausen, *Inorg. Chem.* **1991**, *30*, 96.

[53] In fact, the borinic acids $(2,4,6\text{-}^{i}Pr_3\text{-}C_6H_2)_2BOH$ and $(2,4,6\text{-}(CF_3)_3\text{-}C_6H_2)_2BOH$ lead to the formation of dinuclear homoleptic barium complexes stabilised respectively by intramolecular $Ba\cdots C_\pi$ and $Ba\cdots F$ secondary interactions. By contrast, **2** and its related catalytically active species in the Ba-mediated dehydrocoupling of $\{(Me_3Si)_2CH\}_2BOH$ and hydrosilanes are devoid of such stabilising interactions. The structural investigations performed for a variety barium-boryloxides are beyond the scope of the present study and will be detailed in a forthcoming publication.

[54] T. X. Gentner, B. Rösch, K. Thum, J. Langer, G. Ballmann, J. Pahl, W. A. Donaubauer, F. Hampel, S. Harder, *Organometallics* **2019**, *38*, 2485.

[55] T. X. Gentner, B. Rösch, G. Ballmann, J. Langer, H. Elsen, S. Harder, *Angew. Chem., Int. Ed.* **2019**, *58*, 607.

10.1002/chem.201904933

[56] E. Le Coz, H. Roueindeji, T. Roisnel, V. Dorcet, J.-F. Carpentier, Y. Sarazin, *Dalton Trans.* **2019**, *48*, 9173.

10.1002/chem.201904933

Table of Contents

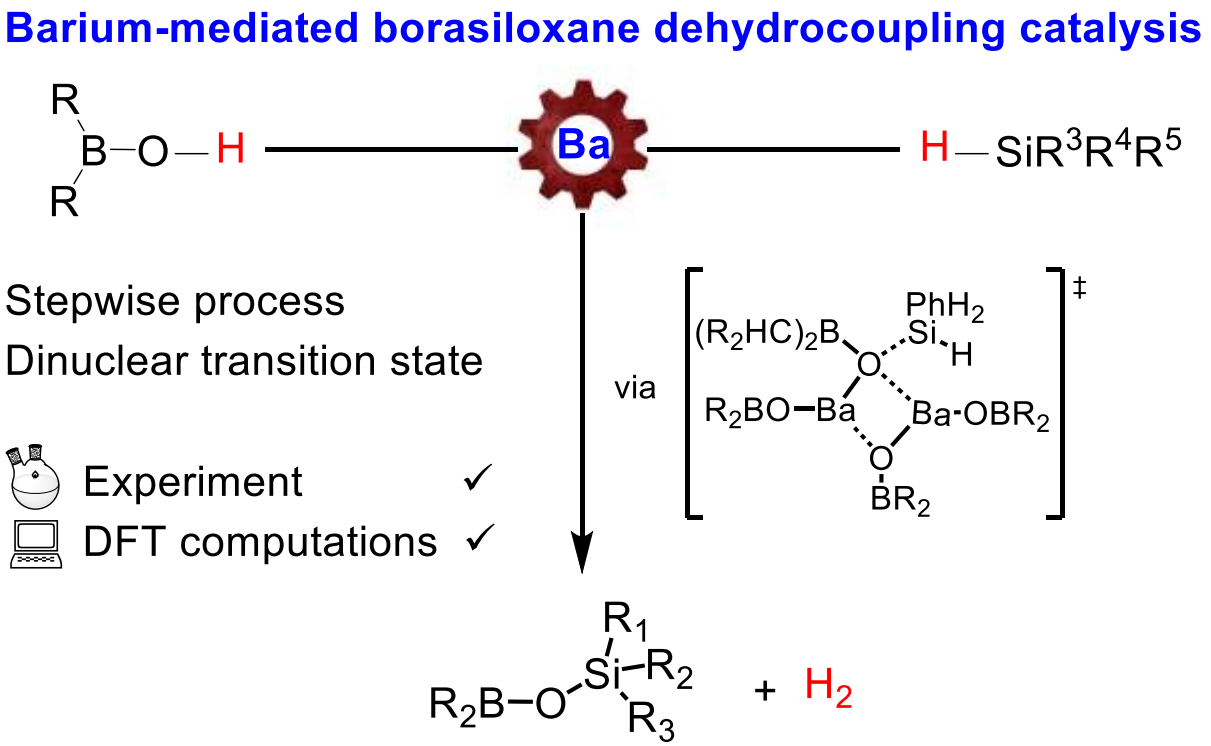

The mechanism of the barium-mediated dehydrocoupling of borinic acids and hydrosilanes, yielding borasiloxanes in controlled fashion, has been established by combined experimental and computational investigations.